

CAV2021

11th International Symposium on Cavitation
May 10-13, 2021, Daejeon, Korea

Ultrasonic cavitation erosion mechanism of free-floating Al₃Zr intermetallics

Abhinav Priyadarshi ^{1*}, Shazamin Bin Shahrani ¹, Tungky Subroto ², Koulis Pericleous ³, Dmitry Eskin ^{2,4},
John Durodola ¹, and Iakovos Tzanakis ^{1,5}

¹ Faculty of Technology, Design and Environment, Oxford Brookes University, Oxford OX33 1HX, United Kingdom

² Brunel Centre for Advance Solidification Technology (BCAST), Brunel University London, Uxbridge UB8 3PH,
United Kingdom

³ Computational Science and Engineering Group (CSEG), Department of Mathematics, University of Greenwich,
London SE10 9LS, United Kingdom

⁴ Tomsk State University, Tomsk 634050, Russia

⁵ Department of Materials, University of Oxford, Oxford OX1 3PH, United Kingdom

Abstract: In this paper, we investigate the cavitation-induced erosion and breakdown mechanism of free-floating Al₃Zr crystals exposed to ultrasonic vibrations in water at different exposure times using in-situ high-speed imaging technique and scanning electron microscopy (SEM). The post-mortem microstructural examination of the damaged crystals shows that the micron-sized hierarchical crack network structure is initially formed in the outer layer of the crystals. Subsequently, the cracked surface undergoes delamination with subsequent layer-by-layer breakdown into micro-fragments in the range of 5-50 μm. This process is accelerated every time the fragment is dragged into the cavitation zone by the recirculating acoustic flow conditions.

Keywords: Ultrasonic melt treatment, cavitation erosion, primary intermetallic crystal, fragmentation, high-speed imaging

1. Introduction

Grain refinement during solidification of Al-alloy melts can be achieved either using chemical inoculation by adding refiners or through dynamic nucleation and multiplication of grains when subjected to an external processing field [1]. The inoculation approach is usually influenced by the formation of a constitutional supercooling zone and the selection of a nucleant [2]. On the other hand, dynamic nucleation and multiplication of solid phases primarily depends on the type of external field applied, i.e. mechanical, electromagnetic or ultrasonic vibration [3–5]. As the chemical inoculation brings along additional solutes and/or impurities, the application of external fields is a more appropriate choice for high-purity Al cast alloys.

Structure refinement using ultrasonic cavitation melt treatment (UST) has gained popularity in casting technology owing to its simple, effective and eco-friendly response during solidification process [6]. The mechanism of grain refinement by ultrasonic processing operate through either cavitation-induced dendritic/crystal fragmentation [3] or cavitation-assisted heterogeneous nucleation [7] through wetting and activation of inclusions [8]. Fragmentation of primary intermetallic crystals has been identified as the most promising method of producing microstructural refinement in Al-based alloys during controlled UST [6,9]. However, understanding the interaction dynamics of cavitation bubbles, ultrasound induced acoustic flow and solidifying intermetallic phases especially at the liquid–solid (L-S) interface in real alloy melts becomes complex, not least owing to real-time observational difficulties caused by the opaqueness of molten metals. Lately, studies related to observations of such highly dynamic phenomena have used water [6,10] and other transparent organic melts [11] to replicate the liquid metal behaviour and monitor the dynamic interaction of bubbles with solid phases.

* Corresponding Author: Abhinav Priyadarshi, abhinav.priyadarshi-2018@brookes.ac.uk

In the present work, experiments were conducted, to study the cavitation erosion mechanism of free-floating primary Al₃Zr intermetallic in de-ionised water upon exposure to high power ultrasound for different treatment durations. The micro-fragmentation behaviour of the crystal was elucidated by means of high-speed imaging and post-mortem SEM observations. The results revealed that ultrasonic treatment of floating crystals lead to severe erosion and breakdown into small size fragments that can act as favourable sites facilitating heterogeneous nucleation and promoting microstructural refinement in real alloy melts.

2. Materials and Methods

Primary Al₃Zr crystals were initially extracted from an Al-3 wt% Zr alloy using the process described in Priyadarshi et al. [10]. Single crystals with dimensions in the range of $4.5 \pm 1 \text{ mm} \times 3.3 \pm 1 \text{ mm} \times 0.06 \pm 0.01 \text{ mm}$ were then exposed to ultrasonic irradiation using a transducer (UP200S, Hielscher Ultrasonics) operating at a frequency of 24 kHz in a transparent vessel of size $25 \text{ mm} \times 10 \text{ mm} \times 45 \text{ mm}$ (L×W×H) containing 4 ml of de-ionised water. The ultrasound was supplied using a titanium built sonotrode ($\varnothing = 3 \text{ mm}$) submerged 10 mm below the liquid surface under ambient conditions. The in-situ fragmentation of an extracted crystal as mentioned above was captured in real-time using a high-speed camera (Photron SA-Z Fast Cam) in-combination with a Navitar 12x adapter lens providing a focussed view of intermetallic disintegration at a working distance of 165 mm. The imaging was carried out at an optimum frame rate of 3000 frames per second (fps) to record the whole sequence of events at resolution of 640×512 pixels, under a visible light background illumination supplied by a GS Vitec Multi LED flash lamp. Figure 1 shows the high speed imaging setup used for capturing the crystal breakdown under the ultrasonic horn. The acoustically induced crystal break-up sequence was repeated with at least five such separate single crystals to check the consistency of results.

Further, post-mortem microscopic analysis of the fragmented crystals obtained after ultrasonic treatment for 3 s, 6 s, and 9 s was conducted using SEM. After each treatment duration, the fragmented crystals were separated from the sonicated liquid using a $2.5 \mu\text{m}$ filter paper. The crystal fragments were then dried in ambient air and preserved for SEM examination.

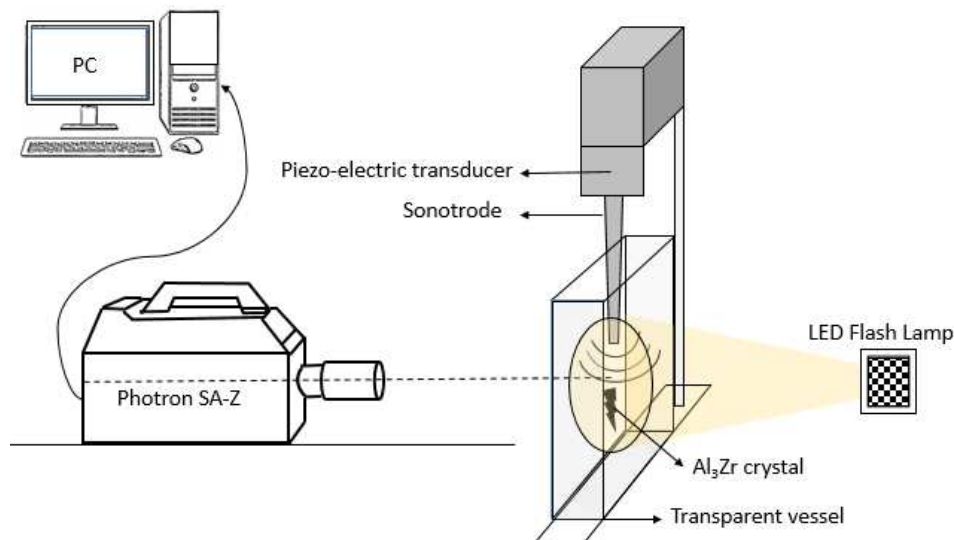


Figure 1. Schematic representation of an in-situ high-speed imaging experimental setup.

3. Results and discussion

3.1. Observation of crystal fragmentation

Figure 2 shows the fragmentation sequence of a free-floating crystal obtained using in-situ imaging. Figure 2a shows a free-floating single intermetallic crystal with dimension as given in section 2 at $t = 0$ ms. The introduction of ultrasonic waves into the liquid drives the crystal towards the vibrating source as shown in Figure 2b due to developed recirculating acoustic flow [12]. As soon as the crystal enters the cavitation zone, it seemingly instantaneously breaks into several small pieces and the fragments are pushed away into the bulk liquid by acoustic streaming (Figure 2c). Acoustic streaming then causes the fragments to recirculate along the marked route as illustrated in Figure 2d. For instance, the fragmented crystal encircled in the black dotted circle can be seen moving back into the intense cavitation zone near the sonotrode in the next frame (Figure 2e). Some of the broken crystals subsequently re-fragment when coming in close proximity of the vibrating probe, where the emitted shock waves are strongest thus causing the fragments to recirculate in a repetitive pattern. The recirculating path varies depending on the momentum acquired by the fragmented crystals (marked in Figure 2f) from the ultrasonic source as shown in Figure 2g. This process then keeps on repeating and the crystal continues to disintegrate via layer-by layer erosion and fragmentation as will be discussed in section 3.2. It is evident from these observations that acoustic streaming is the driver inducing the localised flow causing the crystal that to feed back into the cavitation zone expediting the treatment process. In a real Al melt environment, assuming the acoustic streaming patterns resemble those of the water experiment [6], it is expected that breakdown of these floating primary crystals will be much faster owing to the strong dynamic behaviour of cavitation environment, about 4 times more intense than in water [13], and the aggressiveness of the cavitating field [14,15]. On the other hand, the higher density of the liquid Al will prevent rapid sedimentation of intermetallics and may further facilitate the fragmentation. However, this reasoning is based on preliminary results and is the subject of further research. It has been shown that these crystal fragments will then act as a heterogeneous nucleating sites for Al dendrites ultimately inducing grain refinement in the solidified metallic alloy as will be discussed in the next section [16].

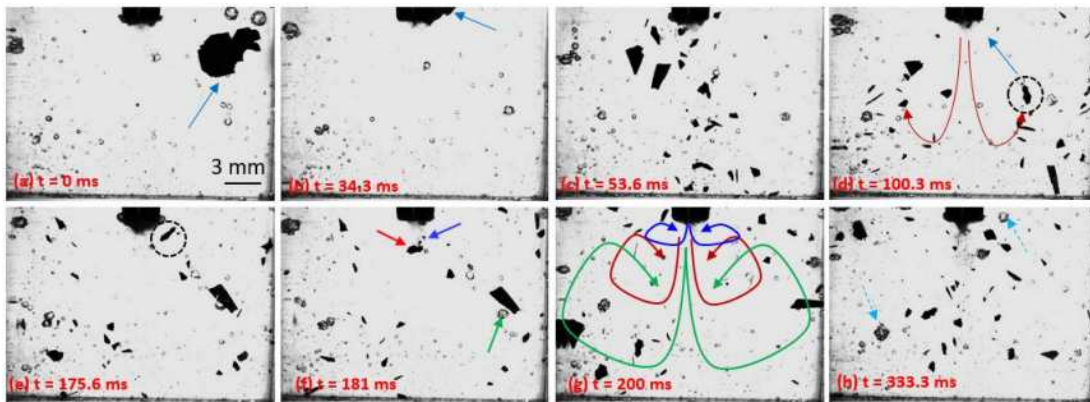


Figure 2. Series of in-situ high-speed images (3000 fps) of ultrasonically induced free-floating crystal breakdown.

3.2. SEM examination of disintegrated primary crystals

Figure 3 shows the morphology of the fragmented intermetallic particles after exposure to the ultrasonic cavitating environment for 3 s, 6 s and 9 s. As shown by our previous research, fragmentation is a result of multiple interactions of shock waves [10] and liquid jets [17] caused by the collapsing bubbles. After 3 s of

treatment, the crystal surface starts to delaminate along the formed crack network structure with crack sizes ranging from 10 to 100 μm as shown in Figure 3a (marked with arrows). It is interesting to note that these fragmented particles show the formation of micron sized crack network along the edges of pre-existing micro crack present on the uppermost layer of the crystal as shown in Figure 3b. Additionally, the fragmented crystals also exhibit various small round shaped blisters projecting out of the surface as evident in Figure 3c. After 6 s, the fragmented crystal undergoes severe cavitation erosion of its upper layer with relatively finer crack network spreading across the whole surface resembling the profile of cracked dried land (Figure 3d). In addition, delamination of the upper layer at specific regions along the surface can be clearly seen in Figure 3e. Furthermore, there is decrease in the density of formed upper layer projections as the majority erode away revealing a crater underneath (Figure 3f). With further increase in the ultrasound exposure i.e. to 9 sec, the crack network becomes even more dense and finer with grid sizes going down to 1-10 μm (Figure 3g). There are almost no visible projections with longer treatment times since the majority must have eroded from the upper layer exposing a large part of the layer beneath (Figure 3h). The top layer is then completely chipped off exposing the layer underneath for further breakdown and disintegration (Figure 3i). As observed from Figure 3, it is obvious that fragmentation of crystal is expedited as exposure time increases. Longer treatment times cause the intermetallic crystal to disintegrate into numerous small fragments in the range of a few microns ideal for promoting heterogeneous nucleation substrates in a real melt [6].

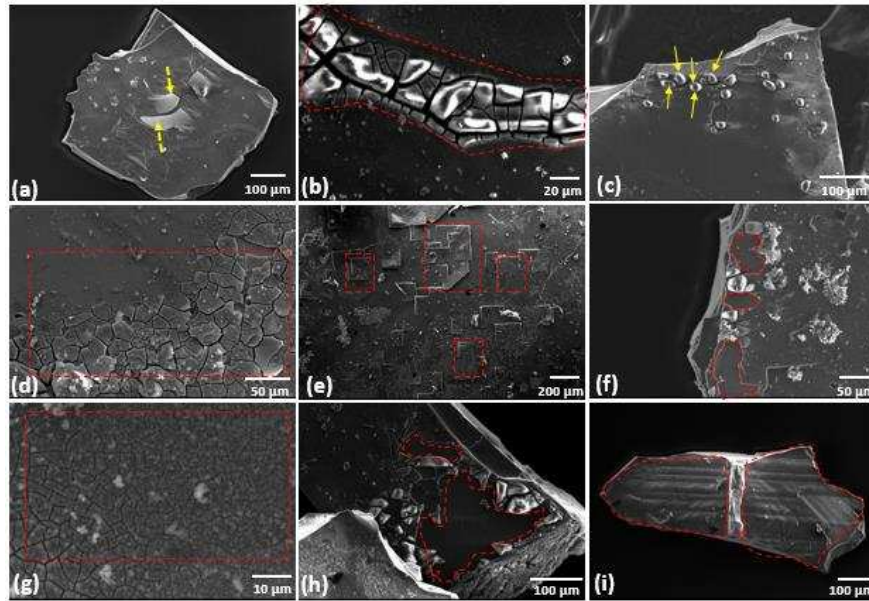


Figure 3. SEM images of fragmented crystal after exposure to ultrasonic cavitation for 3 s (a,b,c), 6 s (d,e,f), and 9 s (g,h,i).

4. Conclusions

Cavitation erosion behaviour of a freely floating single Al_3Zr crystal was qualitatively discussed based on the microstructural examination of the fragmented crystals exposed to different treatment times and in-situ imaging of the entire crystal disintegration dynamics. Exposure to ultrasound first leads to generation of a micron sized hierarchal crack network followed by delamination and fracture in a layer-by-layer manner. Chipped off and protruding fragments are of the size preferable for heterogeneous nucleation in real melts.

CAV2021

11th International Symposium on Cavitation
May 10-13, 2021, Daejeon, Korea

Acknowledgments: This research work has been funded by the UK Engineering and Physical Sciences Research Council (EPSRC) under the project UltraMelt2 (grant EP/R011001/1, EP/R011095/1 and EP/R011044/1).

References

1. Ramirez A, Qian M, Davis B, Wilks T, StJohn DH. Potency of high-intensity ultrasonic treatment for grain refinement of magnesium alloys. *Scr Mater.* 2008, 59(1),19–22.
2. Stjohn DH, Qian M, Easton MA, Cao P. The Interdependence Theory: The relationship between grain formation and nucleant selection. *Acta Mater.* 2011,59(12),4907–21.
3. Eskin GI, Eskin DG. Production of natural and synthesized aluminum-based composite materials with the aid of ultrasonic (cavitation) treatment of the melt. *Ultrason Sonochem.* 2003,10(4–5),297–301.
4. Taghavi F, Saghafian H, Kharrazi YHK. Study on the ability of mechanical vibration for the production of thixotropic microstructure in A356 aluminum alloy. *Mater Des.* 2009,30(1),115–21.
5. Metan V, Eigenfeld K, Rübiger D, Leonhardt M, Eckert S. Grain size control in Al-Si alloys by grain refinement and electromagnetic stirring. *J Alloys Compd.* 2009,487(1–2),163–72.
6. Eskin DG, Tzanakis I, Wang F, Lebon GSB, Subroto T, Pericleous K, et al. Fundamental studies of ultrasonic melt processing. *Ultrason Sonochem.* 2019,52,455–67.
7. Qian M, Ramirez A, Das A, Stjohn DH. The effect of solute on ultrasonic grain refinement of magnesium alloys. *J Cryst Growth.* 2010,312(15),2267–72.
8. Tzanakis I, Xu WW, Eskin DG, Lee PD, Kotsovinos N. In situ observation and analysis of ultrasonic capillary effect in molten aluminium. *Ultrason Sonochem.* 2015,27,72–80.
9. Wang F, Eskin D, Mi J, Wang C, Koe B, King A, et al. A synchrotron X-radiography study of the fragmentation and refinement of primary intermetallic particles in an Al-35 Cu alloy induced by ultrasonic melt processing., *Acta Materialia.* 2017, Vol. 141,142–53.
10. Priyadarshi A, Khavari M, Subroto T, Conte M, Prentice P, Pericleous K, et al. On the governing fragmentation mechanism of primary intermetallics by induced cavitation. *Ultrason Sonochem.* 2021,70,105260-75.
11. Swallowe GM, Field JE, Rees CS, Duckworth A. A photographic study of the effect of ultrasound on solidification. *Acta Metall.* 1989,37(3),961–7.
12. Lebon GSB, Tzanakis I, Pericleous K, Eskin D, Grant PS. Ultrasonic liquid metal processing: The essential role of cavitation bubbles in controlling acoustic streaming. *Ultrason Sonochem.* 2019,55,243–55.
13. Tzanakis I, Lebon GSB, Eskin DG, Pericleous K. Comparison of cavitation intensity in water and in molten aluminium using a high-temperature cavitometer. *J Phys Conf Ser.* 2015,656(1).
14. Tzanakis I, Lebon GSB, Eskin DG, Pericleous KA. Characterisation of the ultrasonic acoustic spectrum and pressure field in aluminium melt with an advanced cavitometer. *J Mater Process Technol.* 2016,229,582–6.
15. Lebon GSB, Tzanakis I, Pericleous K, Eskin D. Experimental and numerical investigation of acoustic pressures in different liquids. *Ultrasonics Sonochemistry.* Vol. 42, 2018,411–21.
16. Atamanenko TV, Eskin DG, Zhang L, Katgerman L. Criteria of Grain Refinement Induced by Ultrasonic Melt Treatment of Aluminum Alloys Containing Zr and Ti. *Metall Mater Trans A [Internet].* 2010,41(8),2056–66.
17. Wang F, Tzanakis I, Eskin D, Mi J, Connolley T. In situ observation of ultrasonic cavitation-induced fragmentation of the primary crystals formed in Al alloys. *Ultrason Sonochem.* 2017,39,66–76.